SAND2019-14961R

Analysis of MARS 2018 Data

B. Cabrera Palmer[1]
(On behalf of the MARS team)
Sandia National Laboratories, 7011 East Avenue, Livermore, CA 94551, USA

(Dated: 9 December 2019)

In this technical note, we present the analysis and results of neutron data collected in 2018 at the Spallation Neutron Source (SNS) by the MARS neutron detector and spectrometer. MARS has been deployed at the SNS "neutrino alley" basement with the purposed of monitoring and characterizing the neutron backgrounds for the COHERENT collaboration. The measured beam neutron rates at the MARS deployment location near some of the COHERENT neutrinos detectors are presented and we discuss what the measured rate and spectra can tell us about the incoming beam neutron flux and energy distribution.

Sandia National Laboratories is a multimission laboratory managed and operated by National Technology & Engineering Solutions of Sandia, LLC, a wholly owned subsidiary of Honeywell International Inc., for the U.S. Department of Energy's National Nuclear Security Administration under contract DE-NA0003525.

I. INTRODUCTION

Understanding the neutron background is of particular importance for experiments aiming to measure coherent elastic neutrino-nucleus scattering (CEvNS) since neutrons produce nuclear recoils similar to the CEvNS signature. For the COHERENT experiment[1] at the Oak Ridge National Laboratory (ORNL) Spallation Neutron Source (SNS), the most important source of neutrons are those precisely produced by the beam at the same time as the neutrinos. Knowledge of the rate and spectral distribution of the beam neutrons reaching the various COHERENT detections system is essential for detector design, modeling and data analysis.

In this technical note, we provide the analysis and results of neutron of neutron data collected by the MARS[2] neutron detector and spectrometer[3] deployed at the SNS with the purpose of monitoring and characterizing the neutron backgrounds for the COHERENT collaboration. Sections (II) and (III) respectively describe the detector and the experimental deployment. Sections (IV) and (V) are devoted to the analysis of the first beam-on MARS dataset collected at the SNS during the year 2018. The measured beam neutron rates at the MARS deployment location near some of the COHERENT neutrino detectors are presented in (V). Although the MARS response studies are still underway, in section (VI) we discuss what the measured rate and spectra can already tell us about the incoming beam neutron flux and energy distribution.

II. MARS DETECTOR

A. Hardware description

The MARS detector consist of twelve BC-408 plastic scintillator layers interleave with Gadolinium coated Mylar sheets. The overall dimensions of the detection volume are $(L \times W \times H) = (75\text{ cm}, 25\text{ cm}, 100\text{ cm})$. This module stands vertically on its $L \times W$ side held by a Unistrut frame, with each $W \times H$ face coupled to a $25 \times 10 \times 100\text{ cm}^3$ acrylic light guide. On each side, eight 5 inch diameter ADIT B133D01 photo multiplier tubes (PMTs) are coupled to the light guides by silicon grease. Black tape covers the scintillator and acrylic volumes for light-tightness, which are further wrapped with an aluminum sheet for fire safety.

B. Electronic read-out and trigger scheme

Data readout is done with two 14 bit, 250 MHz Struck SIS3316 sixteen channel Waveform Digitizers (WFD) mounted in a VME crate. All channels of the first digitizer are used to digitize the sixteen PMT signals. The second digitizer asynchronously records the SNS-provided event-39 and event-61 signals. PMT pairs at the same height but on opposite sides of the scintillator module are joined into the same digitizer's channel group, for a total of four groups. When the sum signal of a four-channel group goes above the digitizer's FIR threshold, the internally generated trigger is routed to the external trigger input, and the sixteen channel waveforms are recorded with a 50-sample pre-trigger window. The raw channel data contain: channel ID, timestamp, peak sample index, peak heigh value, and 6 accumulator sums. Each accumulator stores the integral of 25 samples, with accumulator 0 integrating samples 0-24, accumulator 1 integrating samples 25-49, and so on. At the first stage of processing, the channel integral is calculated as the sum of accumulators 2 to 5 (equivalent to integrating 100 samples) minus the baseline, the latter computed as the average of the first two accumulators (*i.e.*, a 50 sample average). The sum of these sixteen baseline-subtracted integrals is taken to represent the event deposited energy. The time lapses to the previous event-39 signal, previous event-61 signal and the previous event are also computed. A further description of the pre-processed data is given at the start of section (IV).

C. Neutron detection concept

For MARS neutron detection mechanism, we rely on the so-called capture-gated mode. When a fast neutron elastically interacts with Hydrogen atoms in MARS large scintillator volume, the recoiling protons generate a prompt scintillation pulse. If the neutron does not escape, it will bounce around the detector while quickly thermalizing. Given the large Gd thermal neutron capture cross section, there is a high chance that a Gd de-excitation gamma-rays signal will be produced, which have a maximum total energy of ~ 8 MeV. The capture process has a time constant τ_{nCapt} that depends on the Gd concentration, and has been previously measured for MARS to be around 20 μs. Thus, by employing the timing and energy of the Gd gamma-ray scintillation pulses, the population of fully absorbed neutrons

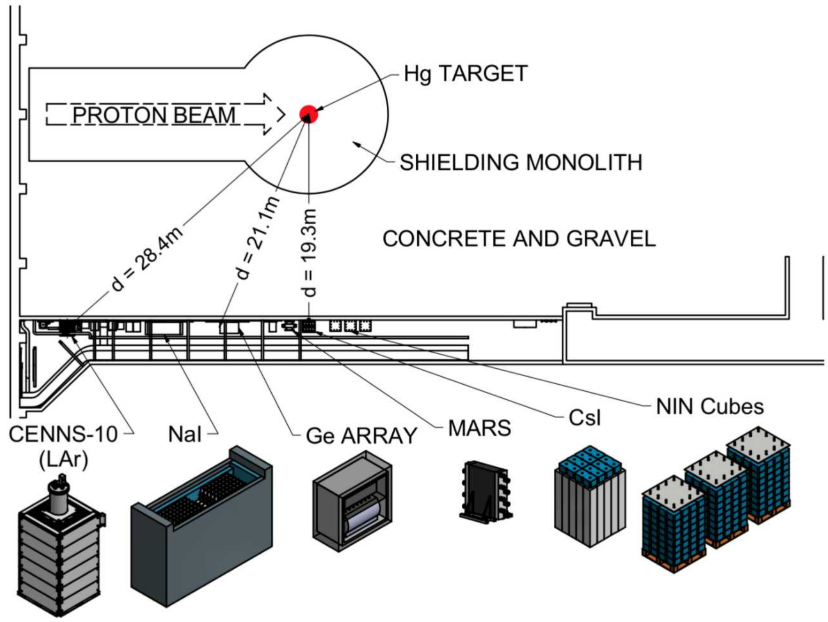

FIG. 1. Detector systems location along the SNS neutrino alley.

can be isolated. Since the neutron's kinetic energy will be fully and quickly transferred to the scintillator, the integral of the prompt pulse is a direct measure of the incoming neutron energy.

III. EXPERIMENTAL DATA

A. Deployment location

In the fall of 2017, MARS was deployed in the SNS basement corridor (the "neutrino alley") next to the CsI[Na] detector system (Fig. 1), at about 20 m from the SNS target, with concrete and gravel filling most of the space from the SNS target and 8 meter water equivalent overburden. A previous neutron background measurement campaign[4] that included 3 different locations along the SNS basement corridor showed the vicinity of the CsI[Na] system as having the lowest SNS beam related neutron background. In this regard, MARS beam-related neutron rates are also expected to be highly suppressed.

A high flux of 511 keV gamma-rays is present all along the neutrino alley. This gamma field originates from a few-inch diameter pipe that runs through the corridor near the concrete ceiling. The pipe carries radioactive gas from the SNS target and creates a high and

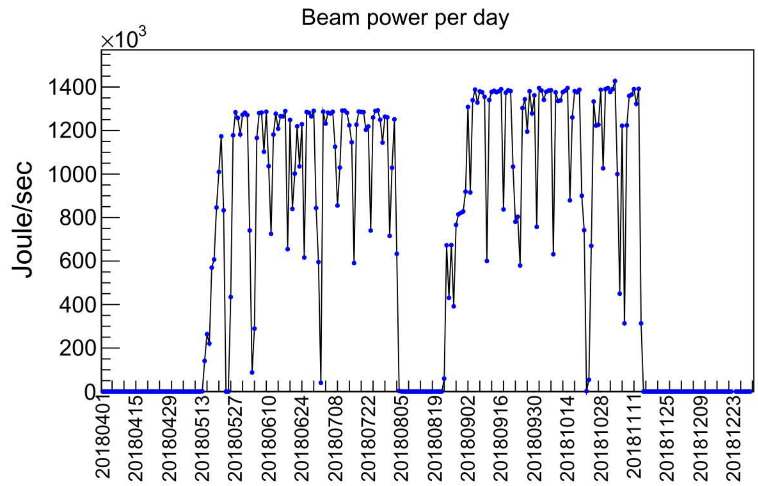

FIG. 2. 2018 SNS delivered beam power.

steadily present "Hot Off Gas" (HOG) background during SNS beam operating periods, and transient background at the SNS start and end operation days. Given that MARS design does not include shielding material of any kind, its response has been found to be highly sensitive to variations in the HOG background during the analyzed period, as will be presented in section (IV). Including high-Z or low-Z shielding material next to MARS would modify the incoming neutron flux that it is supposed to characterize. Thus, efforts are currently underway to tightly surround the HOG pipe with enough lead shield to highly suppress the 511 keV background.

B. Collection period and data quality

MARS stable data collection started at the end of December 2017 during the SNS shutdown period, so that sufficient beam-off data was collected before the SNS beam turned on in the middle of May 2018. The analysis here presented uses data from April 01, 2018 to December 31, 2018. Figure 2 shows the beam power per day during the period under analysis. The beam power during the first beam-on period covering June and July had a nominal maximum value of 1.3 E6 Joules/s, while the maximum delivered power increased to 1.4 E6 Joules/s for the the second beam-on period from September to early November.

Figure 3 contains the MARS trigger rate during the year 2018 as reported in the Grafana MARS monitoring dashboard, showing a significant increase in trigger rate due to the intense HOG gamma background during the two beam-on periods of 2018. The Grafana display

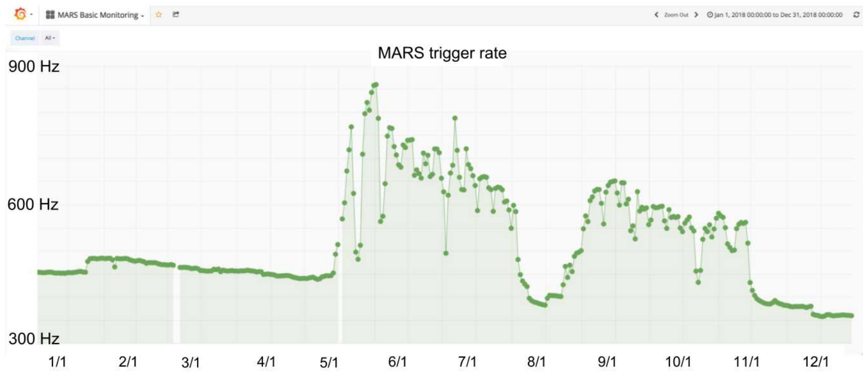

FIG. 3. MARS PMT trigger rate as reported to the Grafana monitoring dashboard.

also clearly shows a decrease in trigger rate during beam-off, likely do to hardware issues that effectively caused an overall gain shift in MARS response. In section (IV 1), we present a gain correction analysis procedure to compensate for this effect.

In Appendix B, we list the pre-processed data files of the period under analysis, which are obtained after initially processing the binary raw data files as will be explained in section (IV). During stable operations, a new run –and thus, a new file– is started every 24 hours. The last column of Appendix B's tables describe observed issues in the data, like interruptions in data collection, missing daily files, variations in file size, individual PMT channel glitches revealed by the Grafana monitoring, etc. These tables also list in detail the data files that will be grouped together when integrating one-week and two-week signal rates in section (IV)'s analysis.

IV. DATA PROCESSING

In data pre-processing, an event is defined as the sequence of 16-PMT sum pulses separated by no more than 200 microseconds. Each event contains the timestamp of the preceding event-39 signal (a ROOT TTimeStamp in units of nanoseconds since EPOCH), the count of event-39 signals within the corresponding run, and an event-61 flag to indicate if there was a beam spill associated with that event-39 signal[5]. These event pulses are grouped in all possible pulse pairs — for example, an event with 3 pulses contains 3 pairs. Each pulse pair is described by the variables (t_1, E_1, dt, E_2), where t_1 is the time interval between the first pulse of the pair, or prompt pulse, and the preceding event-39 trigger (and thus, $t_1 < 1/60$ s), E_1 is the first pulse's baseline-subtracted integral in "adc" units, dt is the inter-pulse time (restricted to be $dt < 200\ \mu s$) and E_2 is the "adc" energy of the second pulse, also called delayed pulse. When a capture-gated neutron detection occurs, (t_1, E_1) represent the prompt neutron thermalization pulse time and energy, while (dt, E_2) represent the decay time and energy of the Gd decay gamma-ray pulse due to the neutron capture. Since the Gd neutron capture time constant in this detector was previously measured to $\sim 20\ \mu$s, setting $dt < 200\ \mu s$ will reject a negligible number of neutron-capture events.

1. Gain correction using Michel electrons

Cosmic muons penetrating MARS can produce large pulses and represent the main contribution to the high-energy end of the light yield spectrum with a bump at around 4×10^5 adc, which correspond to ~40 MeV[6]. Muons decaying within the detector produce highly energetic Michel electrons with a decay time constant[7] of $\tau_{\mu-} = 2.2\ \mu s$ and a spectrum cutoff at ~50 MeV[8]. This type of event also has a double-hit (E_1, E_2) signature corresponding to the muon's ionization E_1 as it traverses the detection medium followed by the Michel electron deposition E_2, and are included in our pairs population. The black histogram of Fig.4's left panel shows the prominent and wide Michel electron E_2 bump obtained by restricting $E_1 > 3 \times 10^5$ adc to represent muon track high energy depositions. The dt profile of these pairs, presented in Fig.4's right panel, agrees with the Michel electron's $\tau_{\mu-}$.

Given the prominence of the Michel electron peak compared to any other MARS spectra features, we use it to monitor gain variations over time and derive a correction. To avoid being affected by the spectral shifts due to the HOG background effect of the pulse integral (see in section (IV 2)), the gain changes are computed only using beam-off data collected sufficiently after the last beam-on day of each beam period. The left panel of Fig.5 shows the effective gain decrease of the August 16-22 beam-off data with respect to the May 7-13 beam-off data. A relative gain correction factor $g_c = 1.04064$ is computed by minimizing the χ^2 between the May 7-13 spectrum and the *gain corrected* August 16-22 spectrum; the latter is also shown in the figure. For the beam-on data comprised between those two weeks, we make the assumption that the gain decreases linearly and compute a daily gain correction by interpolating from $g_c = 1$, on May 7 to $g_c = 1.04064$ on August 16.

Similarly, the right panel of Fig.5 shows the effective gain decrease of the December 3-9 beam-off data with respect to the August 16-22 beam-off data. In this case, the linear gain

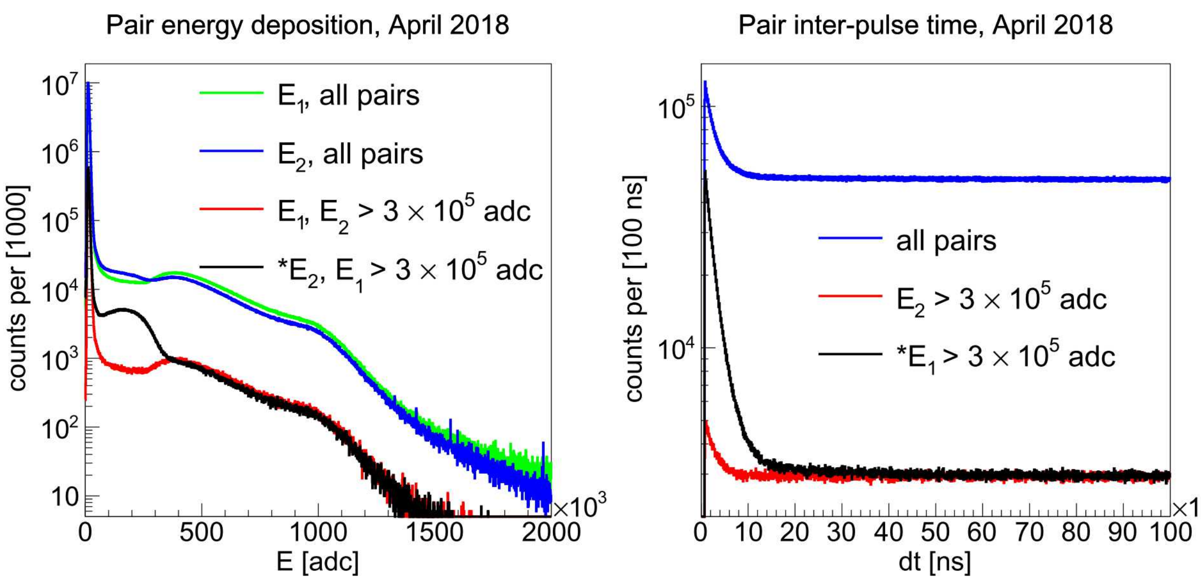

FIG. 4. E_1, E_2 and dt histograms of all pairs from April 2018 beam-off data. By restricting $E_1 > 3 \times 10^5$ adc to represent muon-track high energy depositions, the corresponding E_2 and dt histograms, presented in black, clearly show the the Michel electron spectral and time constant profiles.

correction applied to the second period of beam-on data corresponds to the interpolation from $g_c = 1$, on August 16 to $g_c = 1.02639$ on December 3. Each beam period data is independently corrected relative to its start to restrict the propagation of any systematic error arising from our linear gain correction assumption.

2. E_2 cut selection from the muon-induced neutron events

Cosmic muons produce neutron spallation in the detector and surrounding high-Z materials like the concrete walls. The detection of this neutron population constitute a large steady-state background that can be employed to derive the dt and $E2$ capture-gated cuts for beam neutron detection. As in the case of Michel electrons, the muon-induced neutron interactions are selected by tagging events with “muon track” high energy depositions. While the muon-induced neutrons would produce prompt protons before the Gd neutron-capture gamma-ray emission, we do not observe a useful rate of triple pulse events with the energy and time structure expected from “muon track, prompt proton recoil, Gd gamma-ray shower” events. On the other hand, we detect a useful rate of pulse pairs with $E_1 > 3 \times 10^5$ adc, presumably

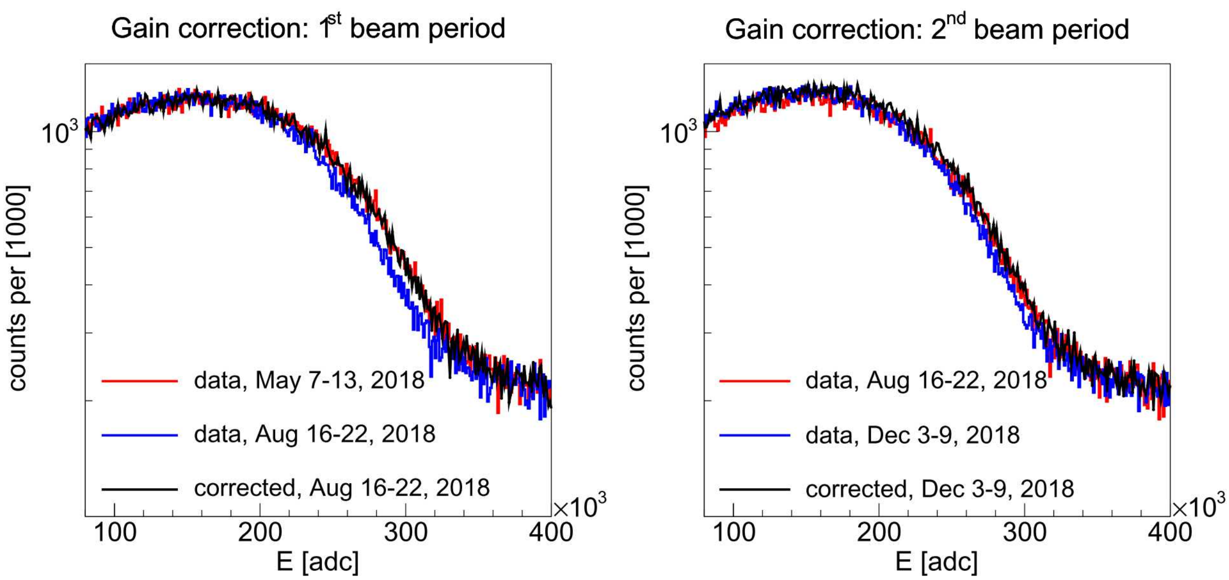

FIG. 5. Michel electron spectrum shift from the start (red) to the end (blue) of each beam-on period due to a gradual hardware gain reduction. The gain-corrected spectrum corresponding to the end of each beam-on period is presented in blue.

corresponding to muon track high energy depositions, followed by E_2 pulses with the dt time structure consistent with neutron capture in Gd. This suggests that the kinetic energy of the muon-related neutrons incident on MARS must fall below our trigger threshold ~ 1 MeVee, or 4 MeV in proton recoil energy[9,10].

Fig.6's left panel contains a "dt vs.E_2" 2D-histogram with the prompt pulse $E_1 > 3 \times 10^5$ adc selected to represent muon tracks. The right panel's dt-projections for two different E_2 ranges show that, while Michel electron events appear to be irreducibly present for both ranges, a second time constant $\tau_{Gd} = 14.78$ μs is present for $E_2 \in [3, 8]8 \times 10^4$ adc corresponding to the presence of muon-induced neutron captures.

Fig.7's left panel shows the E_2-projections for two different dt ranges: a neutron capture dt range (represented in red in Fig.6) starting at $\sim 8\tau_{\mu-}$ in order to reject Michel electron pairs and ending at $\sim 3\tau_{Gd}$, and a second "above-capture" dt range (in black in Fig.6) covering low-rate accidental background pairs. The residual counts between these two histograms are thus interpreted as muon-induced neutron-capture events, and, as expected, show the same rate for a beam-off month (April 2019) and a beam-on month (July 2019). However, as illustrated in Fig.7's right panel, the E_2 values of the beam-on residual counts are shifted up compared to the beam-off E_2 values by 5×10^3 adc, which in light-output energy units

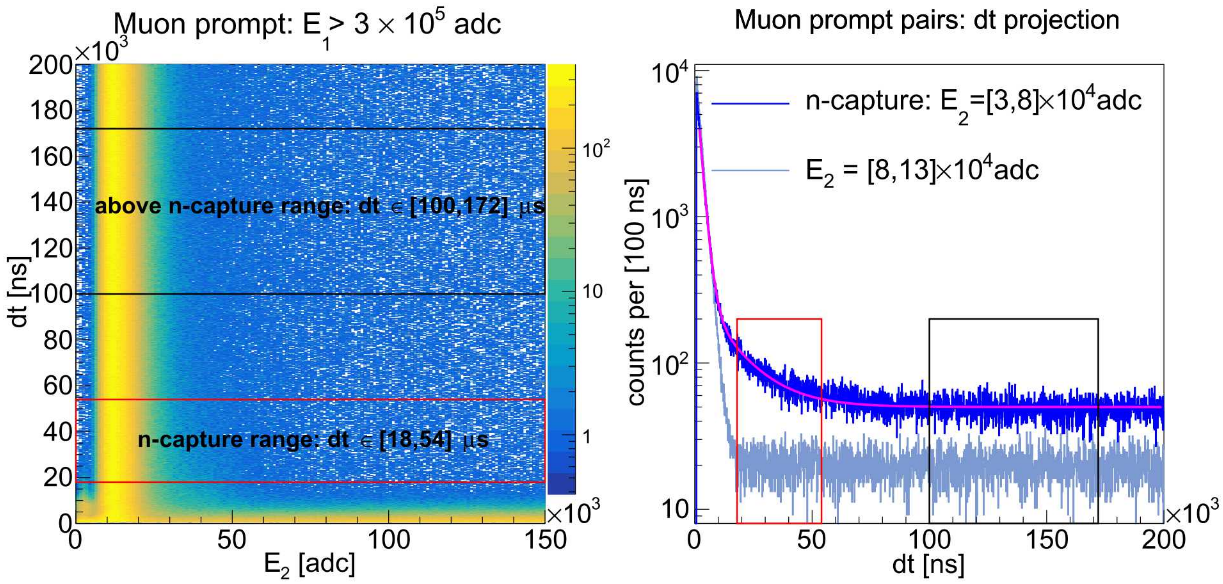

FIG. 6. Left: "dt vs.E_2" 2D-histogram with the prompt pulse $E_1 > 3\times10^5$ adc selected to represent muon tracks, April 2018 beam-off data. Right: dt-projections for two different E_2 ranges. A double exponential fit (pink) of the $E_2 \in [3,8]8\times10^4$ adc dt-projection results in $\tau_{\mu^-} = (2.0447\pm0.0004)\ \mu s$ and $\tau_{Gd} = (14.78 \pm 0.03)\ \mu s$.

corresponds to about ~ 0.5 MeVee. This systematic increase in the pulse integral values is due to a high pile-up rate of HOG background 511 keV gamma-rays.

The muon-induced neutron-capture counts integrated over one-week data intervals (see Appendix B for details on the data intervals) depend on beam power status when the same E_2 cut is used for beam-off and beam-on data, as can be observed in Fig.8. Since the number of muon-induced neutron events produced in MARS should be independent of beam power, we employ them to adjust the E_2 neutron-capture cuts for each one-week data interval. As the reference one-week rate, we select the average of five beam-off weeks from April 1 to May 6 with reference cuts $dt^{\rm ref} \in [18, 54]\ \mu s$ and $E_2^{\rm ref} \in [25, 75] \times 10^4$ adc. We use the above-capture range $dt^{\rm bkg} \in [100, 172]\ \mu s$ in the "dt vs.E_2" 2D-histogram to estimate the mean accidental background 1D-histogram as a function of E_2 bin, which is then subtracted from the "dt vs.E_2" 2D-histogram. The dt-projection of the background-subtracted 2D-histogram for a given $E2$ range is then integrated within $dt^{\rm ref} \in [18, 54]\ \mu s$ to estimate the muon-induced neutron-capture net counts. Fig.9 shows the background-subtracted dt-projections for the reference beam-off data and for one week of beam-on data. The adjusted cut $[E_2^{\rm min}, E_2^{\rm max}]$

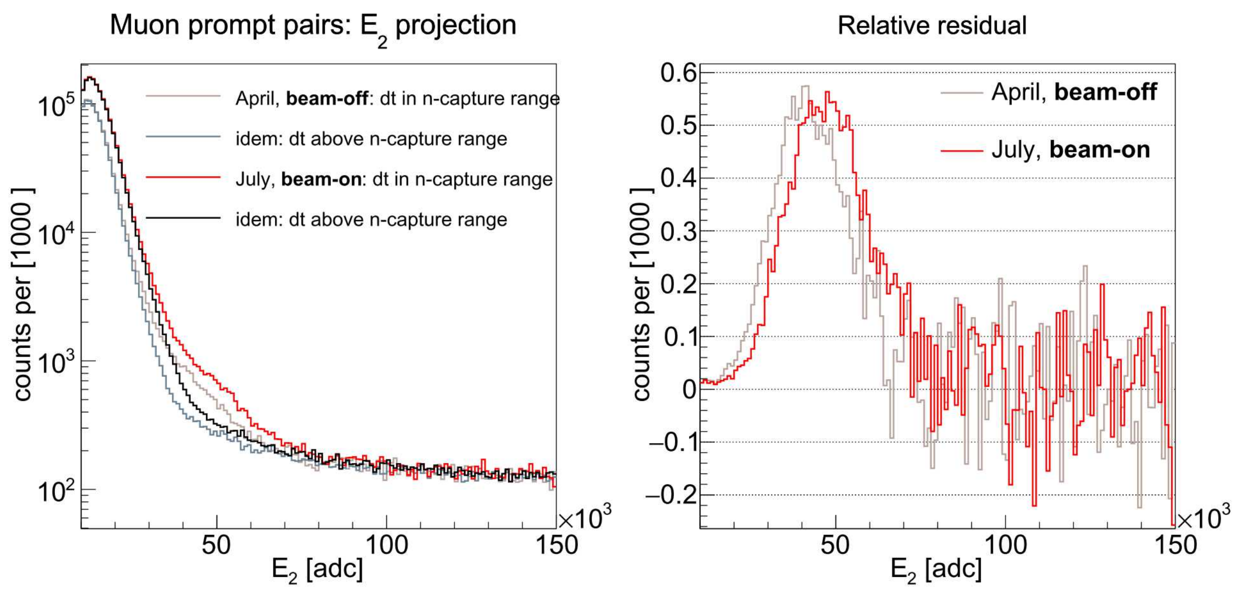

FIG. 7. Right: E_2-projections for the two dt ranges highlighted in Fig.6's left panel, for the April 2018 beam-off and the July 2018 beam-on data. Left: residual counts between the two projections normalized by the n-capture projection bin content, for the April 2018 beam-off and the July 2018 beam-on data.

is derived for each week by minimizing the χ^2 between the reference and the corresponding one-week dt-projection histograms, summing over the dt bins within $dt^{\rm ref}$, and keeping a fixed range width $E_2^{\rm max} - E_2^{\rm min} = 50 \times 10^3$ adc.

The one-week net counts after adjusting the E_2 cuts per week are shown in Fig.10 together with the counts for a fixed E_2 cut. Similar graphs for two-week data intervals are shown in Fig.11. These results demonstrate that the calculated E_2 cuts appropriately offset the spectrum shifting effect due to the HOG background pile-up and therefore can be used to compute the beam-induced neutron rates.

V. BEAM NEUTRON RESULTS

The SNS-target neutrons produced during beam spills that reach MARS will interact within a 2 μs "beam" time window $T_{\rm beam}$, preceded by an event-39 signal that has been advanced in software by 800 μs. Thus, the beam-neutron candidate pairs are constrained by $t_1 \in T_{\rm beam} = [800.0, 802.0]$ μs]. The beam-on data t_1 histograms of Fig.12 clearly shows the beam neutron spike at $T_{\rm beam}$ for pairs with dt and E_2 within cuts consistent with Gd

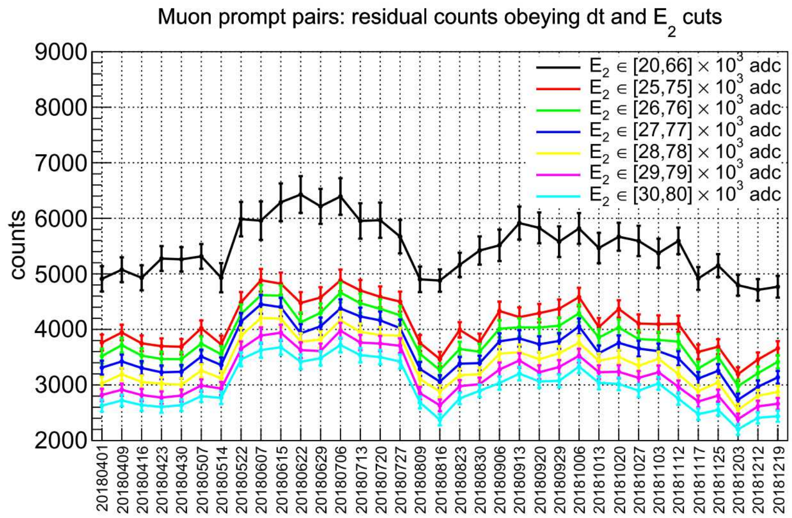

FIG. 8. Muon-induced neutron-capture net counts integrated over one-week data intervals for same E_2 cuts used for the beam-off and beam-on weeks.

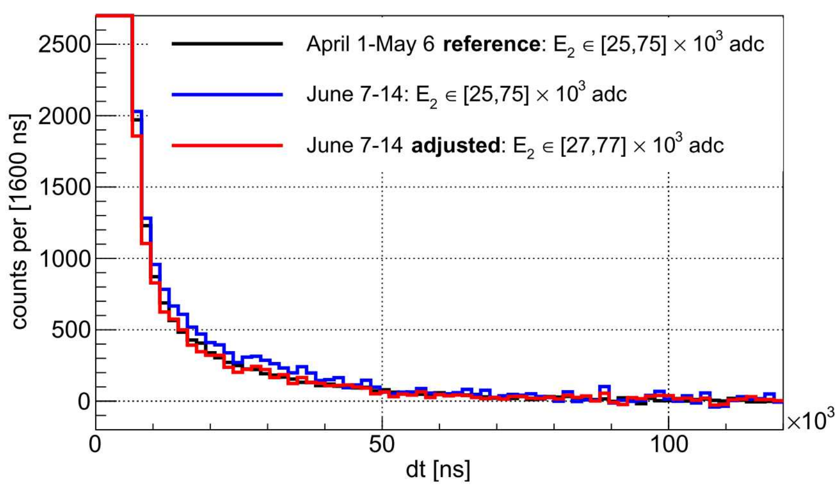

FIG. 9. Background-subtracted dt-projections of muon prompt pairs from April 1-May 6 beam-off and June 7-14 beam-on data. The June 7-14 dt-projection for the adjusted E_2 cuts matches the April 1-May 6 reference dt-projection.

neutron capture. Zooming closer to $T_{\rm beam}$ (Fig.12, right panel) reveals a beam neutron spike with FWHM$\sim$ 300 ns, suggesting that a tighter time bound on beam neutrons could be considered. In order to estimate the steady-state background events in $T_{\rm beam}$, we compute the number of pairs in a long out-of-beam strobe window $t_1 \in T_{\rm strobe} = [1, 15]\ ms$, which is justified by the flat count profile within that window as observed in Fig.12. A third 2 μs out-

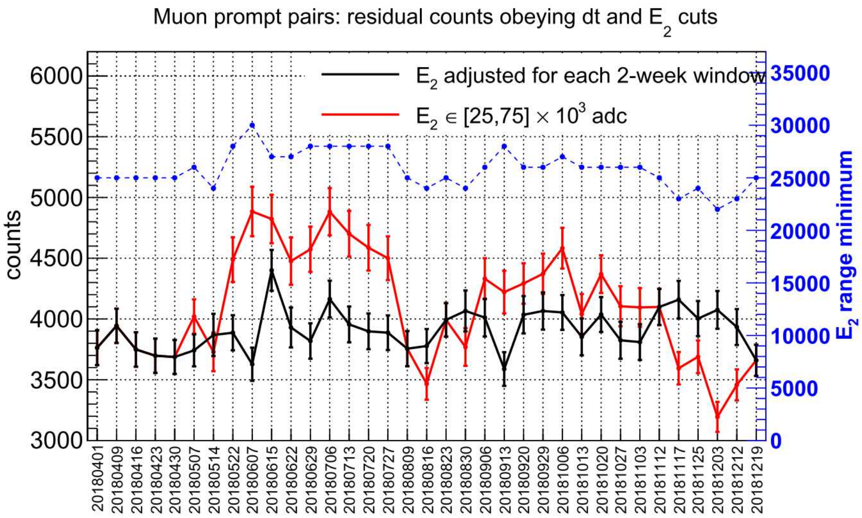

FIG. 10. Muon-induced neutron-capture counts integrated over one-week intervals for E_2 cuts adjusted to maintain a "constant" event count. As a comparison, the counts for a fixed E_2 cut is also plotted. The E_2 range minimum adjusted for each one-week interval are plotted in blue.

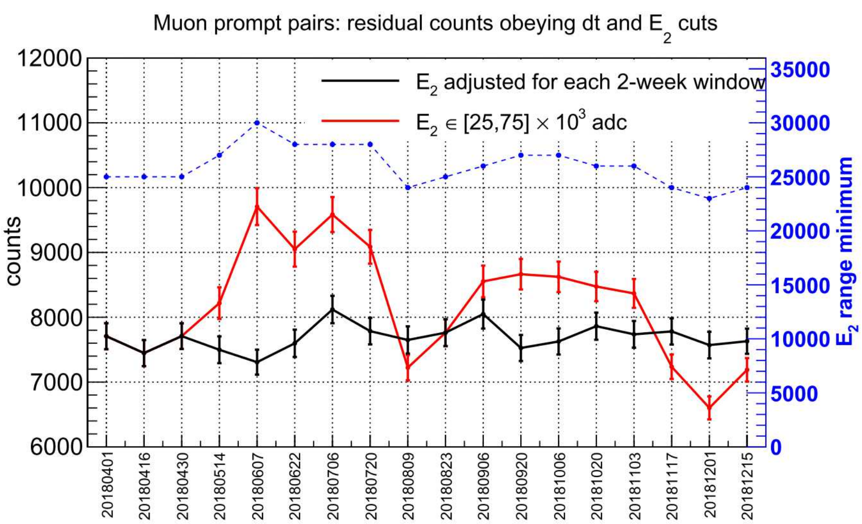

FIG. 11. Muon-induced neutron-capture counts integrated over two-week intervals for E_2 cuts adjusted to maintain a "constant" event count. As a comparison, the counts for a fixed E_2 cut is also plotted. The E_2 range minimum adjusted for each two-week interval are plotted in blue.

of-beam window $T_{\text{check}} = [1000.0, 1002.0]\ \mu s$ is used as a check that steady-state background statistical fluctuations cannot explain the T_{beam} neutron pair excess obtained below.

Figure 13 shows the two-week interval counts for t_1 restricted to time windows T_{beam}, T_{strobe} and T_{check} respectively, dt within the Gd neutron capture cut $dt^{\text{nCapt}} = [6, 54]\ \mu s$, and

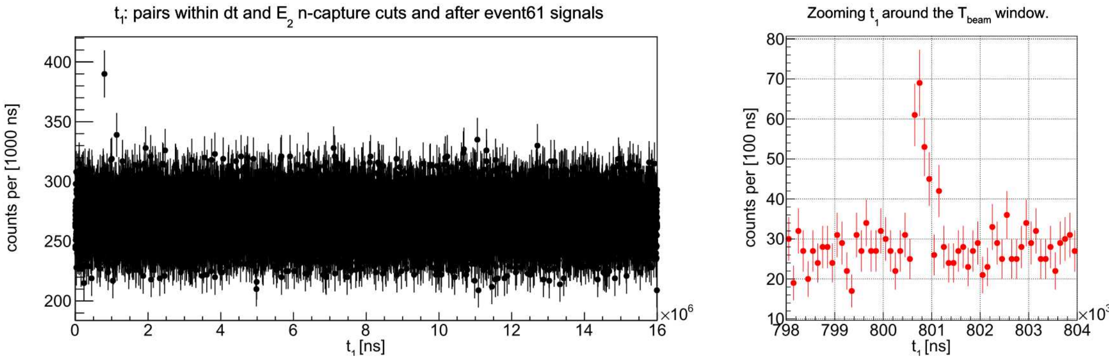

FIG. 12. t_1 histogram for event pairs with $dt \in dt^{\mathrm{nCapt}} = [6, 54]$ μs, satisfying the two-week adjusted E_2^{nCapt} cuts, and with a preceding event-61 signal, from May-December 2018 data.

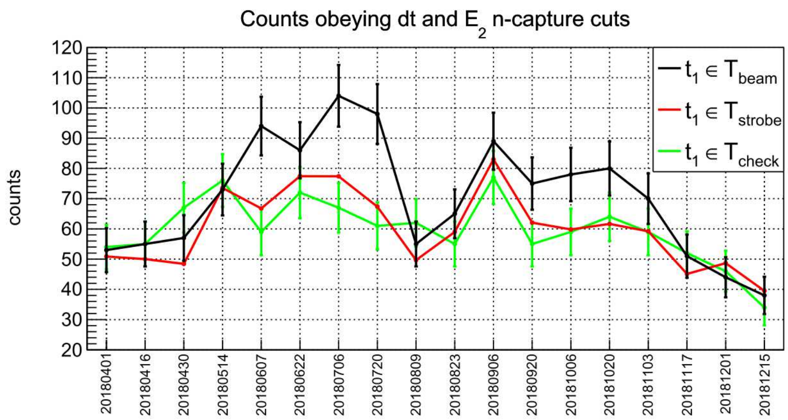

FIG. 13. The two-week interval counts for event pairs with $dt \in dt^{\mathrm{nCapt}} = [6, 54]$ μs, satisfying the two-week adjusted E_2^{nCapt} cuts and t_1 restricted to time windows T_{beam}, T_{strobe} and T_{check}. The T_{strobe} counts have been scaled by $T_{\mathrm{beam}}/T_{\mathrm{strobe}}$. Error bars are statistical.

E_2 obeying the two-week adjusted E_2^{nCapt} cuts described in section (IV 2). Here, the E_2 values have already been corrected for hardware gain shifts as described in section (IV 1). To estimate the steady-state background contribution during the beam window, the T_{strobe} counts have been scaled by $T_{\mathrm{beam}}/T_{\mathrm{strobe}}$. For both beam operating periods (May/14-August/5 and August/23-November/17), the total counts in T_{beam} are consistently larger than the average background counts estimated from T_{strobe}. The counts in T_{check} are, on the other hand, consistent with background fluctuations.

The residual between the T_{beam} counts and the scaled T_{strobe} counts, representing our estimate of the beam neutron counts in MARS, is presented in the top panel of Fig.14. Since the beam neutron rate is expected to be correlated with proton-on-target (POT) power, the counts in Fig.14's middle panel have been normalized by the total beam energy delivered during each corresponding two-week data integration interval; if the delivered energy is zero, the beam-energy normalized counts are set to zero. To account for variability in the data integration time length, Fig.14's bottom panel presents the counts normalized instead by the exact duration of each data integration interval. Figure 15 shows the total beam energy (in Joules), the total number of event-61 triggers and the duration (in seconds) of each two-week interval.

Figures 16 and 17 present the dt and E_2 histograms for all the 2018 data, after applying the Gd neutron capture cuts E_2^{nCapt} and dt^{nCapt} respectively, and for the three t_1 windows under consideration. The "T_{beam}" histograms consistently show event excesses within the respective neutron capture regions, compared to the background histograms for the T_{strobe} and T_{check} windows. The dt residual excess, shown in Fig.16's bottom panel, seems to extend only up to ~ 30 ns, which is shorter than the dt^{nCapt} cut. Similarly, the E_2 residual excess seems to end somewhere around 60×10^3 adc, also shorter than all the adjusted E_2^{nCapt} ranges. Thus, further optimization of the t_1, dt and $E2$ cuts could potentially reduce the neutron-beam signal sensitivity to background statistical fluctuations.

Lastly, Fig.18's top panel show the deposited prompt energy E_1 for all the 2018 data satisfying the Gd neutron capture cuts. The E_1 residual excess during T_{beam}, presented in Fig.18's bottom panel, does not extend beyond $\sim 70 \times 10^3$ adc, which approximately correspond to 7 MeVee, or 13 MeV in proton recoil energy.

VI. CONCLUSIONS

For this data, we recorded 164.8 ± 30.2 neutron counts in 154 beam-on days when the total delivered beam energy was 1.39245×10^{13} Joules. For about 5.184×10^6 beam spills per day, we get an average of 0.207×10^{-6} neutrons per spill. Previous work[3] estimated MARS capture-gated mode neutron detection efficiency to be $\sim 1.25 \times 10^{-1}$ m^2 for any neutron energy. Thus, the incoming neutron flux is estimated to be 1.65×10^{-6} neutron/m^2/spill, which is consistent with the previously measured bounds on the neutrino alley beam neutron flux. As seen above, we do not observe a significant incoming neutron spectrum flux above ~ 13 MeV.

These results demonstrate that the MARS detector is able to monitor the very low beam

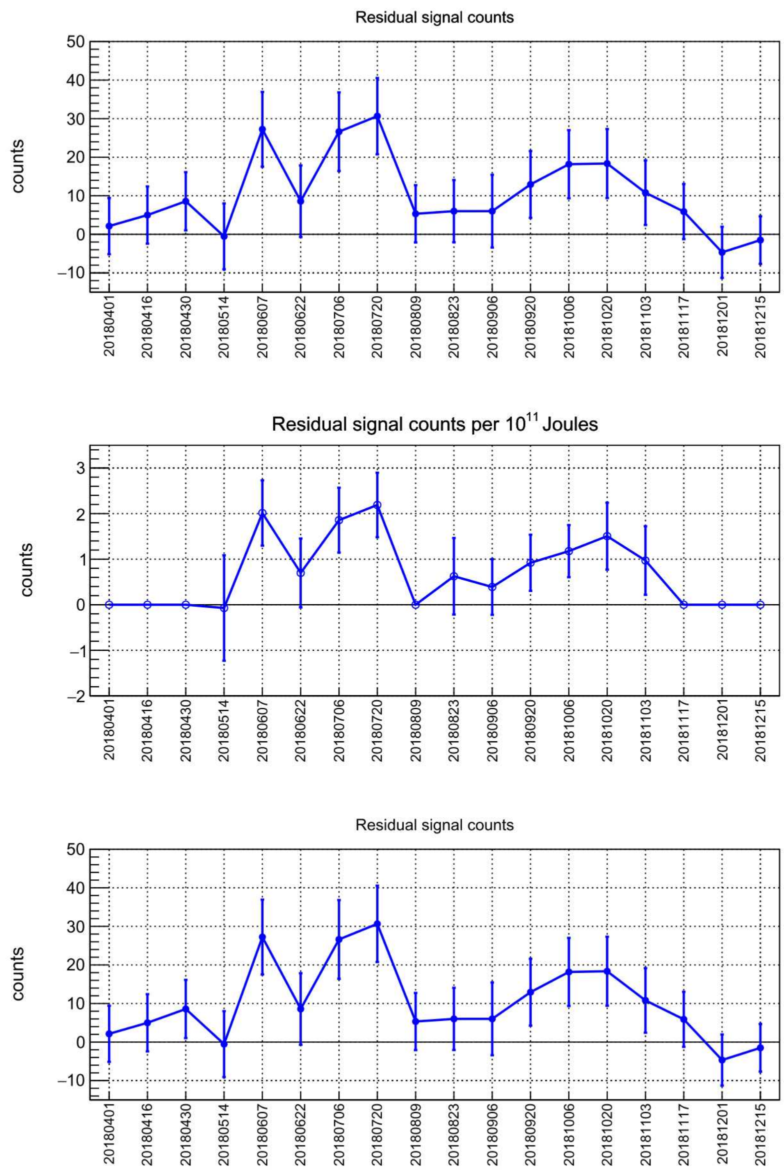

FIG. 14. Top: the two-week interval residual between the T_{beam} counts and the scaled T_{strobe} counts. Middle: residual counts normalized by the total beam energy delivered during each corresponding two-week data integration interval. Bottom: residual counts normalized by the exact duration of each data integration interval. Error bars are statistical.

neutron flux at the neutrino alley under nominal SNS operations: a four week data integration yields a mean of 30 beam neutron counts with about 43 % error at the quietest neutrino alley location. Thus, a 25 % error characterization of beam neutron fluence at several locations along the neutrino alley can be done by keeping MARS at each location for

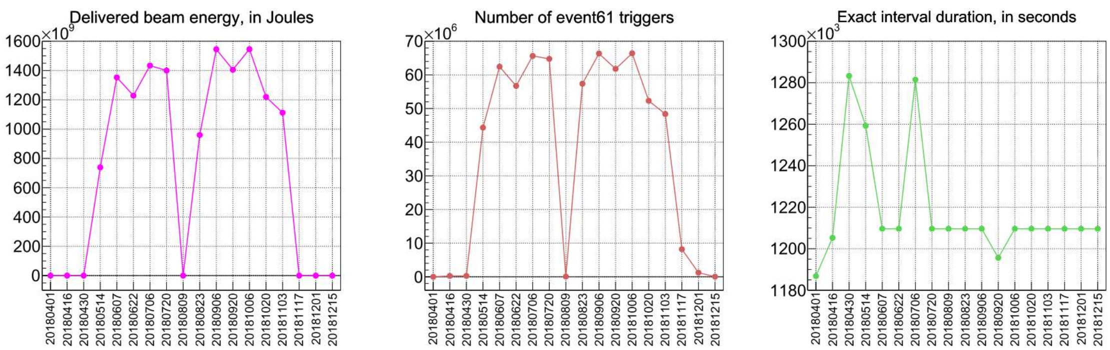

FIG. 15. The total beam energy (in Joules), the total number of event-61 triggers and the duration (in seconds) of each two-week interval.

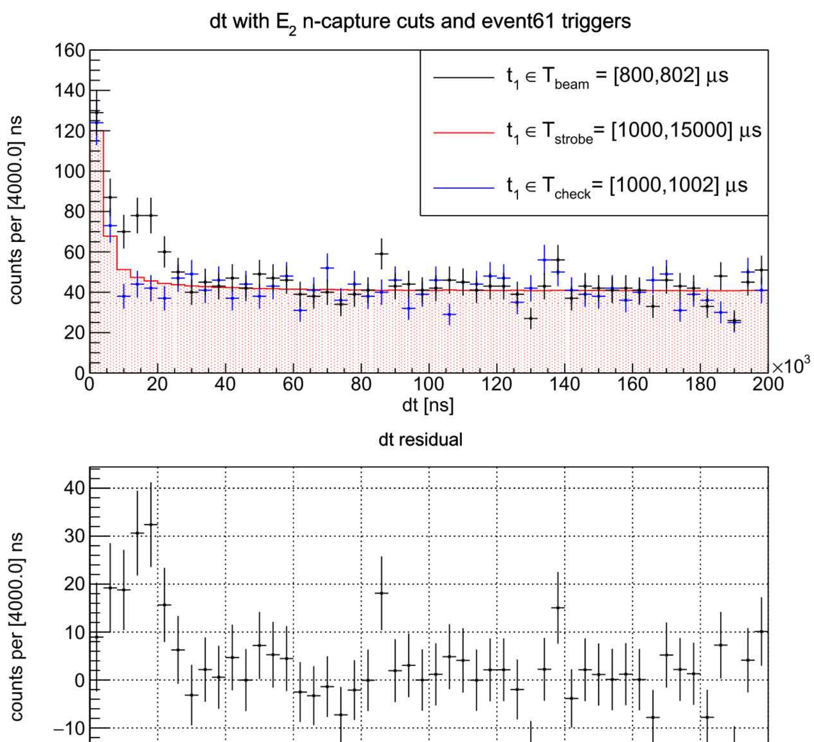

FIG. 16. Top: the dt histogram for event pairs satisfying the two-week adjusted E_2^{nCapt} cuts and with a preceding event-61 signal, from May-December 2018 data. Bottom: residual between the T_{beam} and the T_{strobe} histograms.

three beam-on months at a time. On the other hand, sensitivity to beam power variations similar to the 7 % difference in nominal beam power between the two 2018 beam periods

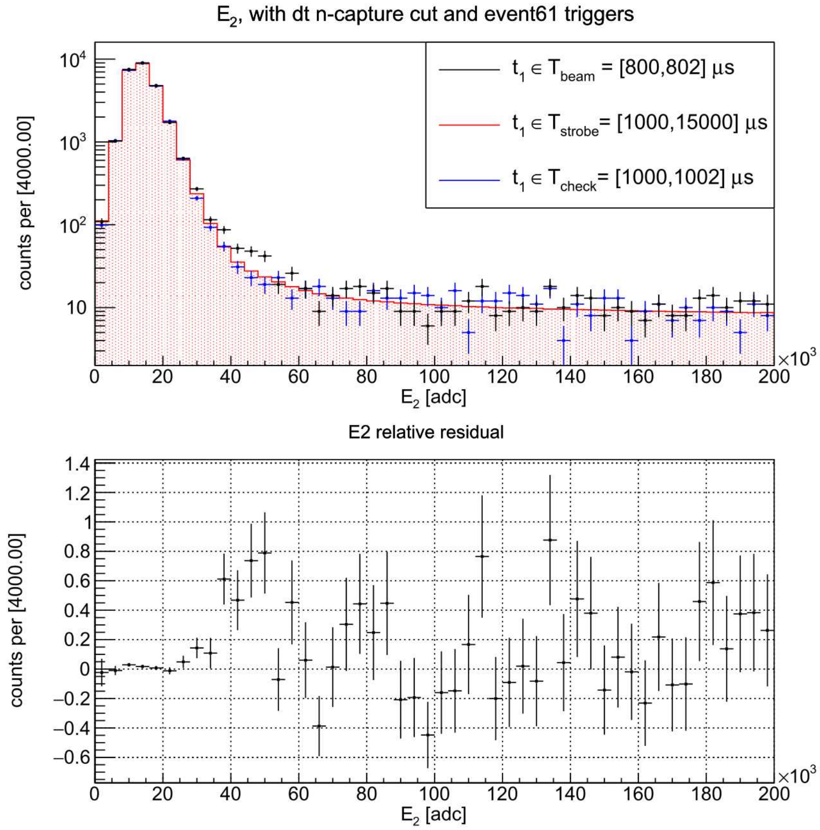

FIG. 17. The E_2 histogram for event pairs with $dt \in dt^{\mathrm{nCapt}} = [6, 54]$ μs and with a preceding event-61 signal, from May-December 2018 data. Bottom: residual between the T_{beam} and the T_{strobe} histograms, normalized by the T_{beam} histogram bin content.

would require about 2.9 years of data under the current background and analysis cuts.

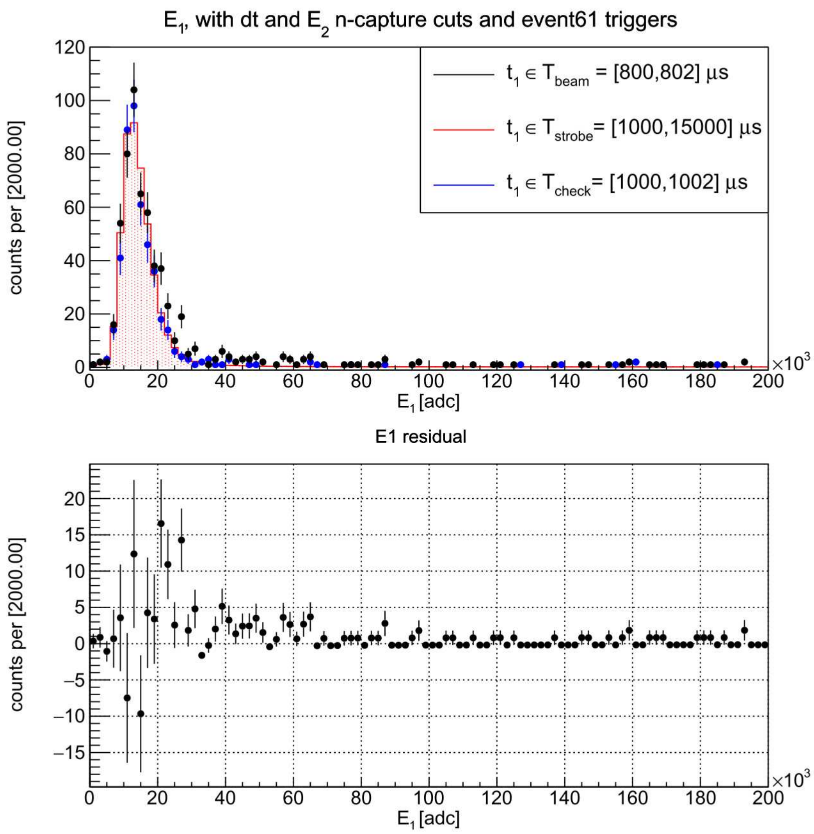

FIG. 18. The E_1 histogram for event pairs with $dt \in dt^{\rm nCapt} = [6, 54]$ μs, satisfying the two-week adjusted $E_2^{\rm nCapt}$ cuts, and with a preceding event-61 signal, from May-December 2018 data. Bottom: residual between the $T_{\rm beam}$ and the $T_{\rm strobe}$ histograms.

ACKNOWLEDGMENTS

Sandia National Laboratories is a multimission laboratory managed and operated by National Technology and Engineering Solutions of Sandia, LLC, a wholly owned subsidiary of Honeywell International Inc., for the U.S. Department of Energy's National Nuclear Security Administration under contract DE-NA0003525.

Appendix A: Significance

To quantize the signal-to-noise ratio of the 2018 data under the chosen analysis cuts, we compute the significance S_0 defined as

$$S_0 = \frac{T - (T_{\text{beam}}/T_{\text{strobe}})S}{\sqrt{T + (T_{\text{beam}}/T_{\text{strobe}})^2 S}} = \frac{T - B}{\sqrt{\sigma_T^2 + \sigma_B^2}} \tag{A1}$$

where T is the neutron-capture pair counts — $dt \in dt^{\text{nCapt}} = [6, 54]\ \mu s$ and E_2 obeying the two-week adjusted E_2^{nCapt}— with $t_1 \in T_{\text{beam}}$, and S is the neutron-capture counts with $t_1 \in T_{\text{strobe}}$, and $B = (T_{\text{beam}}/T_{\text{strobe}})S$ in the estimated mean background in T_{beam}. The two-week interval values of S_0 for our current neutron-capture cuts are presented in Fig.19.

A slightly higher significance $\tilde{S}_0$, shown in Fig.20, is obtained for tighter neutron capture cut $\tilde{dt}^{\text{nCapt}} = [6, 30]\ \mu s$ and the two-week adjusted $\tilde{E}_2^{\text{nCapt}}$ cuts modified so that E_2^{min} are not changed, but $\tilde{E}_2^{\text{max}} = E_2^{\text{min}} + 35 \times 10^3$adc. The overall significance from all the beam-on data for the two neutron capture cuts are $S_0^{\text{all}} = 5.46$ and $\tilde{S}_0^{\text{all}} = 5.93$ respectively. The result is consistent with our above observation that the residual counts of Figures 16 and 17 seem to have a shorter range than the cuts used in this analysis.

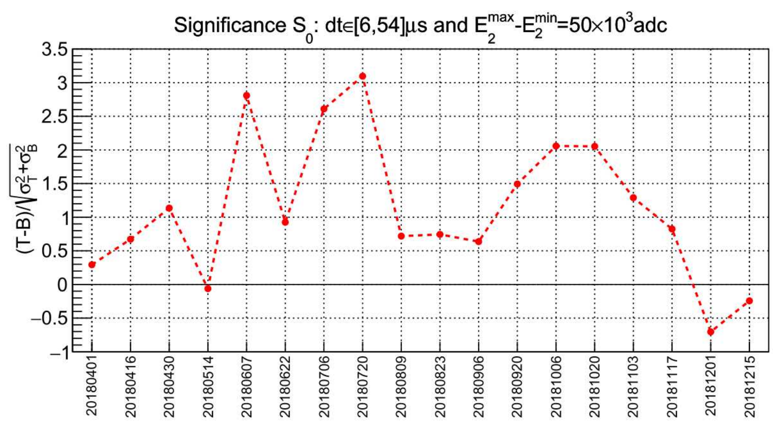

FIG. 19. Significance $S = (T - B)/\sqrt{\sigma_T^2 + \sigma_B^2}$, for $dt \in dt^{\text{nCapt}} = [6, 54]\ \mu s$ and the two-week adjusted E_2^{nCapt} cuts where $E_2^{\text{max}} - E_2^{\text{min}} = 50 \times 10^3$adc. Here T is the total counts with $t_1 \in T_{\text{beam}}$ and B in the estimated mean background in T_{beam}.

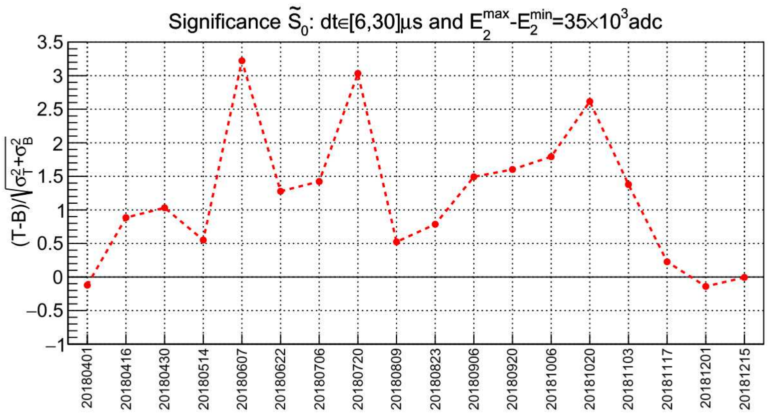

FIG. 20. Significance $S = (T - B)/\sqrt{\sigma_T^2 + \sigma_B^2}$, for $dt \in \tilde{dt}^{\text{nCapt}} = [6, 30]$ μs and the two-week adjusted $\tilde{E_2}^{\text{nCapt}}$ cuts modified so that E_2^{min} are not changed, but $\tilde{E_2}^{\text{max}} = E_2^{\text{min}} + 35 \times 10^3$adc. T and B are defined in Fig.19

Appendix B: Pre-processed data log and date selection for signal integration

TABLE I: One-week and Two-week Selection for rate integration, April to October 2018

Size	File Name	Skip	Notes
— Week 20180401 — Biweek 20180401—			
468M	mars_Evt_20180401220838.root		
468M	mars_Evt_20180402220839.root		
469M	mars_Evt_20180403220840.root		
469M	mars_Evt_20180404220841.root		
467M	mars_Evt_20180405220842.root		
479M	mars_Evt_20180406220843.root	skipped	File runs very slowly
469M	mars_Evt_20180407220844.root		
468M	mars_Evt_20180408220845.root		
— Week 20180409 —			
468M	mars_Evt_20180409220846.root		
467M	mars_Evt_20180410220847.root		
467M	mars_Evt_20180411220848.root		

346M	mars_Evt_20180412220849.root		Short file
2.4M	mars_Evt_20180413220850.root		Data interruption and extra file for 20180413
461M	mars_Evt_20180413223904.root		
462M	mars_Evt_20180414223905.root		
463M	mars_Evt_20180415223906.root		
— Week 20180416 — Biweek 20180416—			
462M	mars_Evt_20180416223907.root		
461M	mars_Evt_20180417223908.root		
460M	mars_Evt_20180418223909.root		
458M	mars_Evt_20180419223910.root		
459M	mars_Evt_20180420223911.root		
459M	mars_Evt_20180421223912.root		
436M	mars_Evt_20180422223913.root		
— Week 20180423 —			
460M	mars_Evt_20180423212758.root		
460M	mars_Evt_20180424212759.root		
459M	mars_Evt_20180425212800.root		
460M	mars_Evt_20180426212801.root		
459M	mars_Evt_20180427212802.root		
458M	mars_Evt_20180428212803.root		
457M	mars_Evt_20180429212804.root		
— Week 20180430 — Biweek 20180430—			
380M	mars_Evt_20180430212805.root		
23M	mars_Evt_20180501173721.root		Data interruption and extra file 20180501
439M	mars_Evt_20180501184654.root		
457M	mars_Evt_20180502184655.root		
456M	mars_Evt_20180503184656.root		
464M	mars_Evt_20180504184657.root		
462M	mars_Evt_20180505184658.root		
454M	mars_Evt_20180506184659.root		

— Week 20180507 —			
453M	mars_Evt_20180507184700.root		
462M	mars_Evt_20180508184701.root		
457M	mars_Evt_20180509184702.root		
465M	mars_Evt_20180510184703.root		
464M	mars_Evt_20180511184704.root		
465M	mars_Evt_20180512184705.root		
466M	mars_Evt_20180513184706.root		
— Week 20180514 — Biweek 20180514—			
471M	mars_Evt_20180514184707.root		
504M	mars_Evt_20180515184708.root		
308M	mars_Evt_20180516184709.root		
334M	mars_Evt_20180518001138.root		No file on 20180517
2.1K	mars_Evt_20180518150206.root		Data interruption and extra file 20180518
610M	mars_Evt_20180519150207.root		
674M	mars_Evt_20180520150208.root		
722M	mars_Evt_20180521150209.root		
— Week 20180522 —			
774M	mars_Evt_20180522150210.root		
617M	mars_Evt_20180523150211.root		
506M	mars_Evt_20180524150212.root		
186M	mars_Evt_20180525150213.root		
492K	mars_Evt_20180526000919.root		Short file
8.7K	mars_Evt_20180526001152.root		Data interruption and extra file 20180526
2.1K	mars_Evt_20180526001320.root		Data interruption and extra file 20180526
711M	mars_Evt_20180527001321.root		
Skipped Data			
802M	mars_Evt_20180528001322.root	skipped	
823M	mars_Evt_20180529001323.root	skipped	Larger file size

810M	mars_Evt_20180530001324.root	skipped	idem
849M	mars_Evt_20180531001325.root	skipped	idem
865M	mars_Evt_20180601001326.root	skipped	idem
866M	mars_Evt_20180602001327.root	skipped	idem
803M	mars_Evt_20180603001328.root	skipped	idem. h_E2_E1MuonRange peak at E2 150E3 adc. Grafana: large baseline stdDev
571M	mars_Evt_20180604001329.root	skipped	
577M	mars_Evt_20180605001330.root	skipped	idem
643M	mars_Evt_20180606001331.root	skipped	idem
— Week 20180607 — Biweek 20180607—			
750M	mars_Evt_20180607001332.root		
771M	mars_Evt_20180609001334.root		No file on 20180608
729M	mars_Evt_20180610001335.root		
717M	mars_Evt_20180611001336.root		
695M	mars_Evt_20180612001337.root		
682M	mars_Evt_20180613001338.root		
733M	mars_Evt_20180614001339.root		
— Week 20180615 —			
730M	mars_Evt_20180615001340.root		
743M	mars_Evt_20180616001341.root		
744M	mars_Evt_20180617001342.root		
744M	mars_Evt_20180618001343.root		
681M	mars_Evt_20180619001344.root		
679M	mars_Evt_20180620001345.root		
686M	mars_Evt_20180621001346.root		
— Week 20180622 — Biweek 20180622—			
662M	mars_Evt_20180622001347.root		
716M	mars_Evt_20180623001348.root		
698M	mars_Evt_20180624001349.root		

709M	mars_Evt_20180625001350.root		
668M	mars_Evt_20180626001351.root		
667M	mars_Evt_20180627001352.root		
722M	mars_Evt_20180628001353.root		
— Week 20180629 —			
723M	mars_Evt_20180629001354.root		
716M	mars_Evt_20180630001355.root		
671M	mars_Evt_20180701001356.root		
636M	mars_Evt_20180702001357.root		
503M	mars_Evt_20180703001358.root		
622M	mars_Evt_20180704001359.root		
673M	mars_Evt_20180705001400.root		
— Week 20180706 — Biweek 20180706—			
688M	mars_Evt_20180706001401.root		
788M	mars_Evt_20180707001402.root		
708M	mars_Evt_20180708001403.root		
668M	mars_Evt_20180709001404.root		
637M	mars_Evt_20180710001405.root		
636M	mars_Evt_20180711001406.root		
722M	mars_Evt_20180712001407.root		
— Week 20180713 —			
688M	mars_Evt_20180713001408.root		
681M	mars_Evt_20180714001409.root		
668M	mars_Evt_20180715001410.root		
553M	mars_Evt_20180716001411.root		
2.1K	mars_Evt_20180716201250.root		Extra file for 20180716
590M	mars_Evt_20180717201251.root		
659M	mars_Evt_20180718201252.root		
663M	mars_Evt_20180719201253.root		
— Week 20180720 — Biweek 20180720—			

664M	mars_Evt_20180720201254.root		
662M	mars_Evt_20180721201255.root		
642M	mars_Evt_20180722201256.root		
639M	mars_Evt_20180723201257.root		
591M	mars_Evt_20180724201258.root		
641M	mars_Evt_20180725201259.root		
642M	mars_Evt_20180726201300.root		
— Week 20180727 —			
641M	mars_Evt_20180727201301.root		
635M	mars_Evt_20180728201302.root		
611M	mars_Evt_20180729201303.root		
613M	mars_Evt_20180730201304.root		
601M	mars_Evt_20180731201305.root		
555M	mars_Evt_20180801201306.root		
604M	mars_Evt_20180802201307.root		
Skipped Data			
594M	mars_Evt_20180803201308.root	skipped	Last 24-hour file with beam on.
496M	mars_Evt_20180804201309.root	skipped	Grafana: decaying rates show HOG transient
468M	mars_Evt_20180805201310.root	skipped	Grafana: decaying rates show HOG transient
449M	mars_Evt_20180806201311.root	skipped	Grafana: decaying rates show HOG transient
442M	mars_Evt_20180807201312.root	skipped	Grafana: decaying rates show HOG transient
438M	mars_Evt_20180808201313.root	skipped	Grafana: ch 14 with noisy baseline.Ch 13,14,15 reduced rate
— Week 20180809 — Biweek 20180809—			
414M	mars_Evt_20180809201314.root		idem

411M	mars_Evt_20180810201315.root		idem
409M	mars_Evt_20180811201316.root		idem
407M	mars_Evt_20180812201317.root		idem
406M	mars_Evt_20180813201318.root		idem
405M	mars_Evt_20180814201319.root		idem
403M	mars_Evt_20180815201320.root		idem
— Week 20180816 —			
402M	mars_Evt_20180816201321.root		
419M	mars_Evt_20180817201322.root		
421M	mars_Evt_20180818201323.root		
421M	mars_Evt_20180819201324.root		
420M	mars_Evt_20180820201325.root		
426M	mars_Evt_20180821201326.root		
422M	mars_Evt_20180822201327.root		
— Week 20180823 — Biweek 20180823—			
427M	mars_Evt_20180823201328.root		Beam ramping up on 201824
443M	mars_Evt_20180824201329.root		
481M	mars_Evt_20180825201330.root		
458M	mars_Evt_20180826201331.root		
484M	mars_Evt_20180827201332.root		
469M	mars_Evt_20180828201333.root		
499M	mars_Evt_20180829201334.root		
— Week 20180830 —			
504M	mars_Evt_20180830201335.root		
507M	mars_Evt_20180831201336.root		
509M	mars_Evt_20180901201337.root		
554M	mars_Evt_20180902201338.root		
584M	mars_Evt_20180903201339.root		
568M	mars_Evt_20180904201340.root		
613M	mars_Evt_20180905201341.root		

— Week 20180906 — Biweek 20180906—			
621M	mars_Evt_20180906201342.root		
633M	mars_Evt_20180907201343.root		
637M	mars_Evt_20180908201344.root		
637M	mars_Evt_20180909201345.root		
608M	mars_Evt_20180910201346.root		
559M	mars_Evt_20180911201347.root		
631M	mars_Evt_20180912201348.root		
— Week 20180913 —			
646M	mars_Evt_20180913201349.root		
651M	mars_Evt_20180914201350.root		
653M	mars_Evt_20180915201351.root		
655M	mars_Evt_20180916201352.root		
634M	mars_Evt_20180917201353.root		
599M	mars_Evt_20180918201354.root		
651M	mars_Evt_20180919201355.root		
— Week 20180920 — Biweek 20180920—			
650M	mars_Evt_20180920201356.root		
614M	mars_Evt_20180921201357.root		
615M	mars_Evt_20180922201358.root		
549M	mars_Evt_20180923201359.root		
471M	mars_Evt_20180924201400.root		Half beam power
595M	mars_Evt_20180927222030.root		No file on 20180925 and 26
599M	mars_Evt_20180928222031.root		
— Week 20180929 —			
598M	mars_Evt_20180929222032.root		
597M	mars_Evt_20180930222033.root		
572M	mars_Evt_20181001222034.root		
573M	mars_Evt_20181002222035.root		

600M	mars_Evt_20181003222036.root		
599M	mars_Evt_20181004222037.root		
598M	mars_Evt_20181005222038.root		
— Week 20181006 — Biweek 20181006—			
600M	mars_Evt_20181006222039.root		
601M	mars_Evt_20181007222040.root		
579M	mars_Evt_20181008222041.root		
554M	mars_Evt_20181009222042.root		
593M	mars_Evt_20181010222043.root		
579M	mars_Evt_20181011222044.root		
580M	mars_Evt_20181012222045.root		
— Week 20181013 —			
578M	mars_Evt_20181013222046.root		
580M	mars_Evt_20181014222047.root		
562M	mars_Evt_20181015222048.root		
550M	mars_Evt_20181016222049.root		
567M	mars_Evt_20181017222050.root		
573M	mars_Evt_20181018222051.root		
579M	mars_Evt_20181019222052.root		
— Week 20181020 — Biweek 20181020—			
565M	mars_Evt_20181020222053.root		
552M	mars_Evt_20181021222054.root		
475M	mars_Evt_20181022222055.root		
453M	mars_Evt_20181023222056.root		
469M	mars_Evt_20181024222057.root		
534M	mars_Evt_20181025222058.root		
558M	mars_Evt_20181026222059.root		
— Week 20181027 —			
552M	mars_Evt_20181027222100.root		
563M	mars_Evt_20181028222101.root		

547M	mars_Evt_20181029222102.root		
558M	mars_Evt_20181030222103.root		
576M	mars_Evt_20181031222104.root		
587M	mars_Evt_20181101222105.root		
582M	mars_Evt_20181102222106.root		

TABLE II: One-week Selection for rate integration, November and December 2018

Size	File Name	Skip	Notes
— Week 20181103—			
579M	mars_Evt_20181103222107.root		
565M	mars_Evt_20181104222108.root		
525M	mars_Evt_20181105222109.root		
516M	mars_Evt_20181106222110.root		
512M	mars_Evt_20181107222111.root		
510M	mars_Evt_20181108222112.root		
555M	mars_Evt_20181109222113.root		
564M	mars_Evt_20181110222114.root	skipped	
569M	mars_Evt_20181111222115.root	skipped	
— Week 20181112—			
569M	mars_Evt_20181112222116.root		
568M	mars_Evt_20181113222117.root		
528M	mars_Evt_20181114222118.root		Beam ramped down on 2018/11/15
446M	mars_Evt_20181115222119.root		Beam off on 2018/11/16
429M	mars_Evt_20181116222120.root		idem
420M	mars_Evt_20181117222121.root		idem. File also in next week selection.
414M	mars_Evt_20181118222122.root		idem. File also in next week selection.
— Week 20181117 —			
420M	mars_Evt_20181117222121.root		idem
414M	mars_Evt_20181118222122.root		idem
411M	mars_Evt_20181119222123.root		idem
408M	mars_Evt_20181120222124.root		Grafana: HOG background transient is done
406M	mars_Evt_20181121222125.root		
405M	mars_Evt_20181122222126.root		
404M	mars_Evt_20181123222127.root		
404M	mars_Evt_20181124222128.root	skipped	

— Week 20181125 —			
406M	mars_Evt_20181125222129.root		Beam on but low. Grafana: small rate spike in rate.
417M	mars_Evt_20181126222130.root		idem
411M	mars_Evt_20181127222131.root		idem
406M	mars_Evt_20181128222132.root		idem
404M	mars_Evt_20181129222133.root		idem
404M	mars_Evt_20181130222134.root		idem
402M	mars_Evt_20181201222135.root		idem
401M	mars_Evt_20181202222136.root	skipped	idem
— Week 20181203 —			
400M	mars_Evt_20181203222137.root		
399M	mars_Evt_20181204222138.root		
400M	mars_Evt_20181205222139.root		
399M	mars_Evt_20181206222140.root		
399M	mars_Evt_20181207222141.root		
399M	mars_Evt_20181208222142.root		
399M	mars_Evt_20181209222143.root		
397M	mars_Evt_20181210222144.root	skipped	
399M	mars_Evt_20181211222145.root	skipped	
— Week 20181212 —			
400M	mars_Evt_20181212222146.root		Grafana: ch 14 with noisy baseline. Ch 13,14,15 reduced rate
384M	mars_Evt_20181213222147.root		idem
383M	mars_Evt_20181214222148.root		idem
383M	mars_Evt_20181215222149.root		idem
381M	mars_Evt_20181216222150.root		idem
380M	mars_Evt_20181217222151.root		idem
381M	mars_Evt_20181218222152.root		idem

— Week 20181219 —			
384M	mars_Evt_20181219222153.root		Grafana: Ch 12,13,14,15 small peak. Ch 14 noisy baseline.
385M	mars_Evt_20181220222154.root		Grafana: ch 14 noisy baseline
383M	mars_Evt_20181221222155.root		idem
382M	mars_Evt_20181222222156.root		idem
383M	mars_Evt_20181223222157.root		idem
383M	mars_Evt_20181224222158.root		idem
383M	mars_Evt_20181225222159.root		idem
— Week 20181226 —			
384M	mars_Evt_20181226222200.root		idem
385M	mars_Evt_20181227222201.root		idem
389M	mars_Evt_20181228222202.root		idem
388M	mars_Evt_20181229222203.root		idem
388M	mars_Evt_20181230222204.root		idem
383M	mars_Evt_20181231222205.root		idem

TABLE III: Two-week Selection for rate integration, November and December 2018

Size	File Name	Skip	Notes
— Biweek 20181103—			
579M	mars_Evt_20181103222107.root		
565M	mars_Evt_20181104222108.root		
525M	mars_Evt_20181105222109.root		
516M	mars_Evt_20181106222110.root		
512M	mars_Evt_20181107222111.root		
510M	mars_Evt_20181108222112.root		
555M	mars_Evt_20181109222113.root		
564M	mars_Evt_20181110222114.root		
569M	mars_Evt_20181111222115.root		
569M	mars_Evt_20181112222116.root		
568M	mars_Evt_20181113222117.root		
528M	mars_Evt_20181114222118.root		Beam ramped down on 2018/11/15
446M	mars_Evt_20181115222119.root		Beam off on 2018/11/16
429M	mars_Evt_20181116222120.root		idem
Biweek 20181117—			
420M	mars_Evt_20181117222121.root		idem
414M	mars_Evt_20181118222122.root		idem
411M	mars_Evt_20181119222123.root		idem
408M	mars_Evt_20181120222124.root		Grafana: HOG background transient is done
406M	mars_Evt_20181121222125.root		
405M	mars_Evt_20181122222126.root		
404M	mars_Evt_20181123222127.root		
404M	mars_Evt_20181124222128.root		
406M	mars_Evt_20181125222129.root		Beam on but low. Grafana: small rate spike in rate.
417M	mars_Evt_20181126222130.root		idem

411M	mars_Evt_20181127222131.root		idem
406M	mars_Evt_20181128222132.root		idem
404M	mars_Evt_20181129222133.root		idem
404M	mars_Evt_20181130222134.root		idem
Biweek 20181201—			
402M	mars_Evt_20181201222135.root		idem
401M	mars_Evt_20181202222136.root		idem
400M	mars_Evt_20181203222137.root		
399M	mars_Evt_20181204222138.root		
400M	mars_Evt_20181205222139.root		
399M	mars_Evt_20181206222140.root		
399M	mars_Evt_20181207222141.root		
399M	mars_Evt_20181208222142.root		
399M	mars_Evt_20181209222143.root		
397M	mars_Evt_20181210222144.root		
399M	mars_Evt_20181211222145.root		
400M	mars_Evt_20181212222146.root		Grafana: ch 14 with noisy baseline. Ch 13,14,15 reduced rate
384M	mars_Evt_20181213222147.root		idem
383M	mars_Evt_20181214222148.root		idem
Biweek 20181215—			
383M	mars_Evt_20181215222149.root		idem
381M	mars_Evt_20181216222150.root		idem
380M	mars_Evt_20181217222151.root		idem
381M	mars_Evt_20181218222152.root		idem
384M	mars_Evt_20181219222153.root		Grafana: Ch 12,13,14,15 small peak. Ch 14 noisy baseline.
385M	mars_Evt_20181220222154.root		Grafana: ch 14 noisy baseline
383M	mars_Evt_20181221222155.root		idem
382M	mars_Evt_20181222222156.root		idem

383M	mars_Evt_20181223222157.root		idem
383M	mars_Evt_20181224222158.root		idem
383M	mars_Evt_20181225222159.root		idem
384M	mars_Evt_20181226222200.root		idem
385M	mars_Evt_20181227222201.root		idem
389M	mars_Evt_20181228222202.root		idem
388M	mars_Evt_20181229222203.root	skipped	idem
388M	mars_Evt_20181230222204.root	skipped	idem
383M	mars_Evt_20181231222205.root	skipped	idem

REFERENCES

[1]D. Akimov, J. B. Albert, P. An, C. Awe, P. S. Barbeau, B. Becker, V. Belov, A. Brown, A. Bolozdynya, B. Cabrera-Palmer, M. Cervantes, J. I. Collar, R. J. Cooper, R. L. Cooper, C. Cuesta, D. J. Dean, J. A. Detwiler, A. Eberhardt, Y. Efremenko, S. R. Elliott, E. M. Erkela, L. Fabris, M. Febbraro, N. E. Fields, W. Fox, Z. Fu, A. Galindo-Uribarri, M. P. Green, M. Hai, M. R. Heath, S. Hedges, D. Hornback, T. W. Hossbach, E. B. Iverson, L. J. Kaufman, S. Ki, S. R. Klein, A. Khromov, A. Konovalov, M. Kremer, A. Kumpan, C. Leadbetter, L. Li, W. Lu, K. Mann, D. M. Markoff, K. Miller, H. Moreno, P. E. Mueller, J. Newby, J. L. Orrell, C. T. Overman, D. S. Parno, S. Penttila, G. Perumpilly, H. Ray, J. Raybern, D. Reyna, G. C. Rich, D. Rimal, D. Rudik, K. Scholberg, B. J. Scholz, G. Sinev, W. M. Snow, V. Sosnovtsev, A. Shakirov, S. Suchyta, B. Suh, R. Tayloe, R. T. Thornton, I. Tolstukhin, J. Vanderwerp, R. L. Varner, C. J. Virtue, Z. Wan, J. Yoo, C.-H. Yu, A. Zawada, J. Zettlemoyer, and A. M. Zderic, "Observation of coherent elastic neutrino-nucleus scattering," Science (2017), 10.1126/science.aao0990, `http://science.sciencemag.org/content/early/2017/08/02/science.aao0990.full.pdf`.

[2]The name MARS stands for Multiplicity and Recoils Spectrometer, and is a legacy from a previous system developed at Sandia National Laboratories and which contained as a module the detector described here.

[3]C. Roecker, A. Bernstein, N. Bowden, B. Cabrera-Palmer, S. Dazeley, M. Gerling, P. Marleau, M. Sweany, and K. Vetter, "Design of a transportable high efficiency fast neutron

spectrometer," Nuclear Instruments and Methods in Physics Research Section A: Accelerators, Spectrometers, Detectors and Associated Equipment **826**, 21 – 30 (2016).

[4]C. Collaboration, D. Akimov, P. An, C. Awe, P. S. Barbeau, P. Barton, B. Becker, V. Belov, A. Bolozdynya, A. Burenkov, B. Cabrera-Palmer, J. I. Collar, R. J. Cooper, R. L. Cooper, C. Cuesta, D. Dean, J. Detwiler, A. G. Dolgolenko, Y. Efremenko, S. R. Elliott, A. Etenko, N. Fields, W. Fox, A. Galindo-Uribarri, M. Green, M. Heath, S. Hedges, D. Hornback, E. B. Iverson, L. Kaufman, S. R. Klein, A. Khromov, A. Konovalov, A. Kovalenko, A. Kumpan, C. Leadbetter, L. Li, W. Lu, Y. Melikyan, D. Markoff, K. Miller, M. Middlebrook, P. Mueller, P. Naumov, J. Newby, D. Parno, S. Penttila, G. Perumpilly, D. Radford, H. Ray, J. Raybern, D. Reyna, G. C. Rich, D. Rimal, D. Rudik, K. Scholberg, B. Scholz, W. M. Snow, A. Sosnovtsev, A. Shakirov, S. Suchyta, B. Suh, R. Tayloe, R. T. Thornton, A. Tolstukhin, K. Vetter, and C. H. Yu, "The coherent experiment at the spallation neutron source," (2015), arXiv:1509.08702 [physics.ins-det].

[5]The float timeSinceEvent61 is set to 100,060 (or 100,064) if there was a beam spill associated with the event-39 trigger.

[6]MARs energy calibrations are not covered in this Technical Note.

[7]K. A. Olive et al. (Particle Data Group), "Review of Particle Physics," Chin. Phys. **C38**, 090001 (2014).

[8]R. Acciarri et al. (MicroBooNE), "Michel Electron Reconstruction Using Cosmic-Ray Data from the MicroBooNE LArTPC," JINST **12**, P09014 (2017), arXiv:1704.02927 [physics.ins-det].

[9]Z. Jian-Fu, R. Xi-Chao, H. Long, L. Xia, B. Jie, Z. Guo-Guang, H. Han-Xiong, and S. Chao-Hong, "Measurements of the light output functions of plastic scintillator using9be(d, n)10b reaction neutron source," Chinese Physics C **34**, 988–992 (2010).

[10]S. A. Pozzi, J. A. Mullens, and J. T. Mihalczo, "Analysis of neutron and photon detection position for the calibration of plastic (bc-420) and liquid (bc-501) scintillators," Nuclear Instruments and Methods in Physics Research Section A: Accelerators, Spectrometers, Detectors and Associated Equipment **524**, 92 – 101 (2004).